A&A 420, 921–927 (2004)
DOI: 10.1051/0004-6361:20035702

Astronomy & Astrophysics

Modelling photoluminescence from small particles

II. Implications for dust rotation and the Extended Red Emission

G. Mulas[1,4], G. Malloci[1,2,4,⋆], and P. Benvenuti[2,3]

[1] INAF – Osservatorio Astronomico di Cagliari – AstroChemistry Group, Strada n.54, Loc. Poggio dei Pini, 09012 Capoterra (CA), Italy
[2] Dipartimento di Fisica, Università degli Studi di Cagliari, S.P. Monserrato-Sestu Km 0.7, 09042 Cagliari, Italy
[3] INAF, Viale del Parco Mellini 84, 00136 Roma, Italy
e-mail: benvenuti@inaf.it
[4] Astrochemical Research in Space Network, http://www.ars-network.org

Received 17 November 2003 / Accepted 9 February 2004

Abstract. The Extended Red Emission (ERE) has been observed in virtually all possible environments in which dust is present, ranging from HII regions to carbon rich planetary nebulae, to reflection nebulae, to dense interstellar clouds, to the diffuse interstellar medium. One problem in comparing ERE with laboratory photoluminescence (PL) measurements is given by the fact that laboratory samples are usually macroscopic in size, or very thin films, while interstellar dust particles are usually of sizes comparable to, or smaller than, the wavelength of visible light. We here apply a newly developed general recipe to extrapolate the expected PL of small, homogeneous spheres starting from the available laboratory results obtained for bulk samples, and infer previously unsuspected consequences for ERE-like PL phenomena.

Key words. astrochemistry – ISM: dust, extinction – ISM: lines and bands – methods: numerical – radiation mechanisms: general – scattering

1. Introduction

The Extended Red Emission (henceforth ERE) is a broad emission whose peak wavelength lies between ~6500 Å and ~8000 Å, with a width of about ~800 Å. It was first discovered in the peculiar Red Rectangle nebula (Schmidt et al. 1980), and almost ten years passed until the spectroscopic detection of a similar feature in many reflection nebulae (Witt & Schild 1988; Witt et al. 1989; Witt & Malin 1989; Witt & Boroson 1990). So far, ERE has been detected also in a dark nebula (Mattila 1979; Chlewicki & Laureijs 1987), in galactic cirrus clouds (Guhathakurta & Tyson 1989; Szomoru & Guhathakurta 1998), in the galactic high latitude diffuse interstellar medium (Gordon et al. 1998), in galactic HII regions (Perrin & Sivan 1992; Sivan & Perrin 1993), in the 30 Doradus nebula in the LMC (Darbon et al. 1998), in a nova (Scott et al. 1994), in carbon rich planetary nebulae (Furton & Witt 1990, 1992), in the halo of the galaxy M 82 (Perrin et al. 1995) and in the Evil Eye galaxy (NGC 4826; M 64) (Pierini et al. 2002). That ERE is a true emission phenomenon and not due to changes in the scattering properties of dust grains, was convincingly proven by Watkin et al. (1991), who showed that the extended red emission was not correlated with the polarisation in the reflection nebula NGC 7023.

If the same agent is supposed to be responsible for the production of ERE in all of these environments, it must be present in a wide variety of kinetic temperature, density and irradiation conditions and it must have a high quantum efficiency for photoluminescence (PL), especially in the diffuse interstellar medium (ISM) (Gordon et al. 1998). Moreover, one of the observed properties of the ERE is that its spectral shape is different even in different positions of the same object, e. g. as in the Red Rectangle, in several reflection nebulae (Witt & Boroson 1990) and in the Orion HII region (Perrin & Sivan 1992).

Several possible carriers for the ERE have been proposed, over the years, to meet these demanding observational constraints. They include gas phase molecules such as Polycyclic Aromatic Hydrocarbons (PAHs) (Léger et al. 1988) and fullerene (C_{60}) and its derivatives (Webster 1993), as well as some solid state components of the interstellar dust, namely various carbonaceous compounds (Duley 1985; Sakata et al. 1992; Seahra & Duley 1999) and pure silicon nanoparticles (Witt et al. 1998; Ledoux et al. 1998, 2001). Each of these hypotheses shows some apparent drawbacks: gas phase fullerenes and derivatives cannot easily reproduce the observed

Send offprint requests to: G. Mulas,
e-mail: gmulas@ca.astro.it
⋆ e-mail: gmalloci@ca.astro.it

continuous spectral variation of ERE; PAHs would necessarily produce the so-called Unidentified Infrared Bands (UIBs) in the near and medium infrared along with ERE, while ERE and the 3.3 μm UIB have been observed not to be always spatially correlated (Perrin & Sivan 1992; Furton & Witt 1992); silicon nanoparticles, due to the very strong dependence of both the quantum efficiency and the peak wavelength of their PL on the size of the crystallites (Ledoux et al. 1998, 2001), would require a very narrow, finely tuned size distribution in order to match ERE in different environments; finally, various flavours of HAC seem to be able to reproduce the full range of PL positions and have the right spectral shape, but not to *simultaneously* match both the spectral distribution of ERE and the required photon conversion efficiency needed to account for the observed ERE in the diffuse ISM, estimated to be near 10% by Gordon et al. (1998). Specifically, HAC needs to be highly hydrogenated to have a high enough PL quantum efficiency, but then its spectrum, *as measured on laboratory samples*, peaks blue-wards of the observed ERE. This leaves us, to date, with no really compelling solution for the ERE enigma.

However, in our previous summary, we emphasised what we believe to be a rather fundamental flaw in the comparisons of the PL by carbonaceous materials and ERE: in stark contrast with the remarkable work on silicon nanoparticles by Ledoux et al. (1998, 2001), in most of the above cited literature laboratory PL measurements on interstellar analogues were made on macroscopic samples or thin films. Interstellar dust is a diluted dispersion of grains of sizes comparable to, or smaller than, the wavelength of the emitted light, probably with a complex structure (core-mantle, fluffy etc.) (see e.g., Mathis & Whiffen 1989; Li & Greenberg 1997). Regardless of their actual shape, such small particles are bound to have optical properties that are very different from those of the bulk material they are made of. Therefore, any attempts to quantitatively compare PL signals from interstellar particles with such experimental data *must* carefully take into account the effect of particle size and optical properties: the difference between the PL properties of bulk samples and those of a small particle may be about as large as that between the respective extinction properties, just for the same reasons. In particular, PL will undergo self-absorption and scattering *within* the material before leaving it, and this effect will be just as different between a dust grain and a bulk sample as absorption and scattering are (Malloci 2003; Malloci et al. 2004). Unless one is considering dust grains that are utterly non-absorbing at the wavelength of the PL, this effect must be properly taken into account and therefore a straight comparison between the spectrum and efficiency of PL in a bulk sample and ERE will yield possibly misleading results.

On the other hand, some theoretical works, such as that by Seahra & Duley (1999) calculate the PL from a very small HAC dust grain as given by the simple superposition of the PL of the constituent aromatic platelets, neglecting any self-absorption effects. While this *may* be appropriate, some more detailed study is in order to assess whether this is indeed the case.

In Malloci et al. (2004), hereafter Paper I, we presented a mesoscopic theory of the PL by small dust grains which enables one to extrapolate laboratory results obtained for bulk samples and obtain the expected PL from small particles made of the same material, very much in the same way as absorption and scattering properties of small dust grains are usually computed using bulk optical "constants".

With specific reference to the ERE phenomenon, we here present a "proof of concept" application of the simple implementation of the above model for homogeneous spheres to a specific HAC flavour obtained as an organic refractory residue produced by UV irradiation of an ice mixture, as described in Jenniskens (1993). The detailed treatment of self-absorption renders the luminescence spectrum dependent both on the size of the dust particle and on the angle between exciting light and the direction of observation, the latter dependence being described by an analytical formula.

Section 2 recalls from Paper I the physics and equations relevant for the present application. In Sect. 3 we discuss the astrophysical implications of the above results, their impact on current hypotheses on the carriers of the Extended Red Emission and their further relevance in testing the rotational properties of interstellar dust particles. Finally, Sect. 4 draws the main conclusions of the present work.

2. The model

In the model developed by Malloci (2003) and Malloci et al. (2004) the elementary PL emission inside a dust particle is represented as an incoherent, unpolarised density of oscillating electric dipoles. This density is assumed to be given by a functional of the energy *locally* absorbed from the exciting radiation field in the neighbourhood of the position of the emitting dipoles. We are here interested in modelling the emission by carbonaceous materials such as HAC, for which the excitation and subsequent luminescence are known to be effectively confined to a single graphitic platelet (Robertson 1996; Seahra & Duley 1999); hence, we will restrict ourselves to the *local* limiting case as described in Malloci (2003) and Malloci et al. (2004). We recall here only the relevant equations.

The PL power $\frac{\mathrm{d}\mathcal{P}_{\mathrm{pl}}}{\mathrm{d}\Omega\mathrm{d}\omega'}$ emitted by a dust grain per unit solid angle and unit frequency interval upon excitation by a monochromatic radiation flux $I(\omega)$, can be written as

$$\frac{\mathrm{d}\mathcal{P}_{\mathrm{pl}}}{\mathrm{d}\Omega\mathrm{d}\omega'} = I(\omega)\left(\frac{\mathrm{d}C_{\mathrm{pl}}}{\mathrm{d}\Omega\mathrm{d}\omega'}\right)_{\mathrm{dust}},$$

where $\frac{\mathrm{d}C_{\mathrm{pl}}}{\mathrm{d}\Omega\mathrm{d}\omega'}$ is the *differential cross section for PL* as defined in Paper I, computed for the assumed geometry of the particle. For the particular case of a homogeneous sphere the above reference provides the following expression:

$$\frac{\mathrm{d}C_{\mathrm{pl}}}{\mathrm{d}\Omega\mathrm{d}\omega'} = \frac{\mathrm{d}\eta_{\mathrm{lab}}}{\mathrm{d}\Omega\mathrm{d}\omega'} \cdot \mathcal{A}(\omega, \omega', a, \theta, \theta_{\mathrm{d}}), \tag{1}$$

where $\frac{\mathrm{d}\eta_{\mathrm{lab}}}{\mathrm{d}\Omega\mathrm{d}\omega'}$ is the experimentally measured PL yield and $\mathcal{A}(\omega, \omega', a, \theta, \theta_{\mathrm{d}})$ is given by

$$\mathcal{A}(\omega, \omega', a, \theta, \theta_{\mathrm{d}}) = \frac{1}{g(\omega, \omega')} \sum_t \gamma_t(a, \omega, \omega') P_t(\cos\theta). \tag{2}$$

The experimentally measured PL yield $\frac{\mathrm{d}\eta_{\mathrm{lab}}}{\mathrm{d}\Omega\mathrm{d}\omega'}$ is the ratio between the measured PL power per unit solid angle and unit

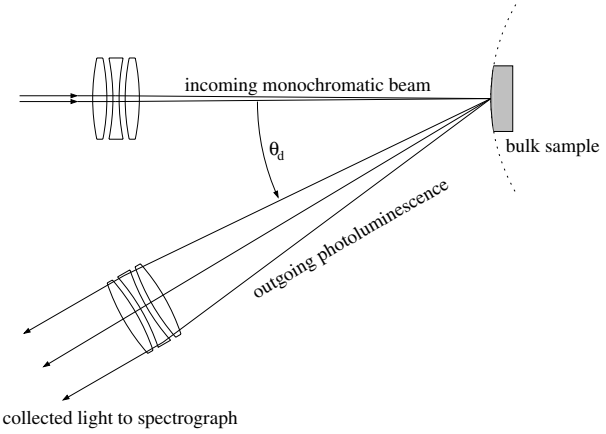

Fig. 1. Schematic description of the experimental setup to measure the PL yield $\frac{d\eta_{lab}}{d\Omega d\omega'}$ on a bulk sample and hence obtain $p_{loc}(\omega, \omega')$ in the local approximation. The sample can be seen as a portion of a sphere of very large radius, represented by the dotted outline.

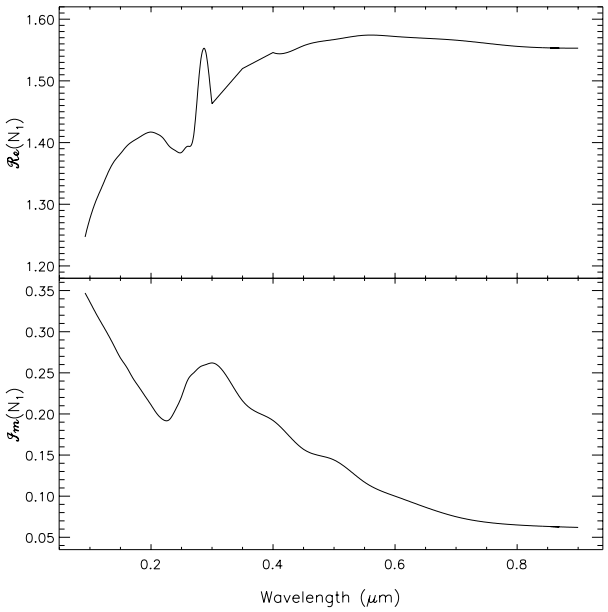

Fig. 2. Real and imaginary part of the refractive index of the processed organic refractory residue, taken from Jenniskens (1993).

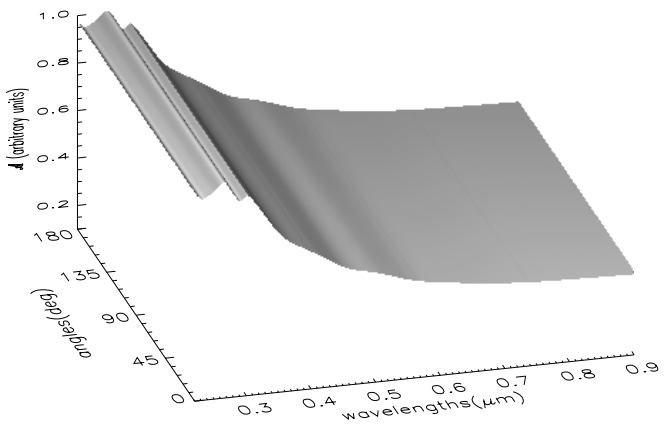

Fig. 3. Form factor $\mathcal{A}(\lambda, \lambda', a, \theta, \theta_d)$: incident wavelength $\lambda = 220$ nm, sphere radius $a = 10$ nm (size parameter $x \sim 0.3$, close to the Rayleigh limit).

frequency in a given direction, as shown in the experimental configuration depicted in Fig. 1, and the power absorbed by the sample from the monochromatic incident exciting light beam. The dependence of $\mathcal{A}(\omega, \omega', a, \theta, \theta_d)$ on the specific laboratory setup used to measure the PL yield is explicitly represented here by the angle θ_d (cf. Fig. 1). In the above equation $g(\omega, \omega')$ is a correction factor, which depends on the experimental setup in which $\frac{d\eta_{lab}}{d\Omega d\omega'}$ was measured, and takes into account self-absorption and scattering within the laboratory sample. The factor $\mathcal{A}(\omega, \omega', a, \theta, \theta_d)$, which has the dimensions of an area, provides the link between the laboratory measure $\frac{d\eta_{lab}}{d\Omega d\omega'}$ and the expected PL for a small, homogeneous sphere. Each P_t is the Legendre polynomial of degree t, and the θ appearing in its argument is the angle between the direction of propagation of the exciting radiation and the direction of observation of the resulting PL emission. The coefficients γ_t depend on the complex refractive index at ω and ω' and on the sphere radius a. The exact definition of $g(\omega, \omega')$ and γ_t can be found in Paper I.

The computed numerical values of the factor $\mathcal{A}(\omega, \omega', a, \theta, \theta_d)$ presented here include only *primary* PL (see Paper I). We computed them using the optical properties, reproduced here in Fig. 2, of the processed organic refractory residue given by Jenniskens (1993).

In Paper I the general behaviour of $\mathcal{A}(\omega, \omega', a, \theta, \theta_d)$ is shown for a sample of frequencies of exciting light and grain sizes, as well as for a different set of optical constants. This demonstrates the impact of particle size effects in modulating the spectral distribution of the PL observed in laboratory experiments performed for bulk samples.

While for a more thorough discussion of the general properties of $\mathcal{A}(\omega, \omega', a, \theta, \theta_d)$ we refer the reader to Paper I, we here summarise the most interesting points from the point of view of ERE interpretation. $\mathcal{A}(\omega, \omega', a, \theta, \theta_d)$ shows a marked dependence both on the wavelength $\lambda' = 2\pi c/\omega'$ of the emitted radiation and on the angle θ between the direction of incident light and the direction of observation. The first dependence is clearly a consequence of the behaviour of the assumed refractive index N_1, which causes increasing self-absorption at smaller wavelengths (see Fig. 2); the second dependence can be seen, in a naïve intuitive way, as an indication of the varying path length that the outgoing light must travel in the absorbing medium before escaping the particle. Both of these dependences display an interference pattern superimposed on a smoother overall behaviour. The interference pattern is strongly dependent both on excitation wavelength and on particle size (see Figs. 3 through 6 in the present work and Figs. 3 through 10 in Paper I), hence it will tend to average out and disappear if one considers either a broad distribution of particle sizes or of exciting wavelengths, or both.

In particular, for an astrophysically relevant example, we here use Eq. (27) of Paper I, assuming monochromatic excitation at 220 nm (near the well known strong absorption feature of carbonaceous materials), a distribution of particle sizes

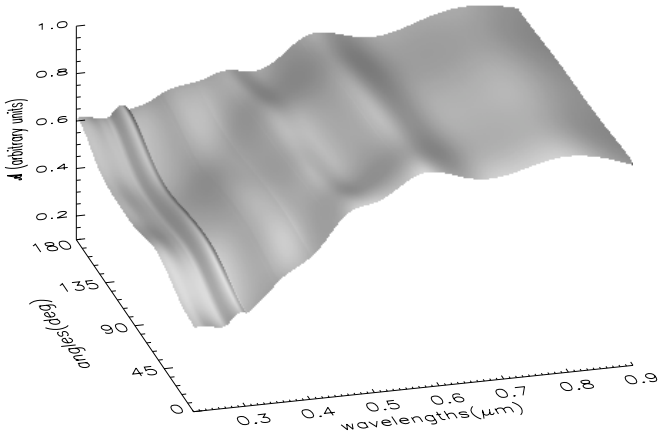

Fig. 4. Form factor $\mathcal{A}(\lambda, \lambda', a, \theta, \theta_d)$: incident wavelength $\lambda = 220$ nm, sphere radius $a = 230$ nm (size parameter $x \sim 6.6$).

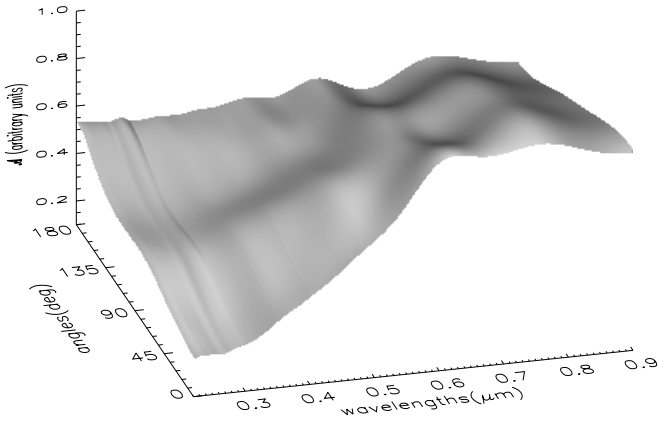

Fig. 5. Form factor $\mathcal{A}(\lambda, \lambda', a, \theta, \theta_d)$: incident wavelength $\lambda = 220$ nm, sphere radius $a = 310$ nm (size parameter $x \sim 8.9$).

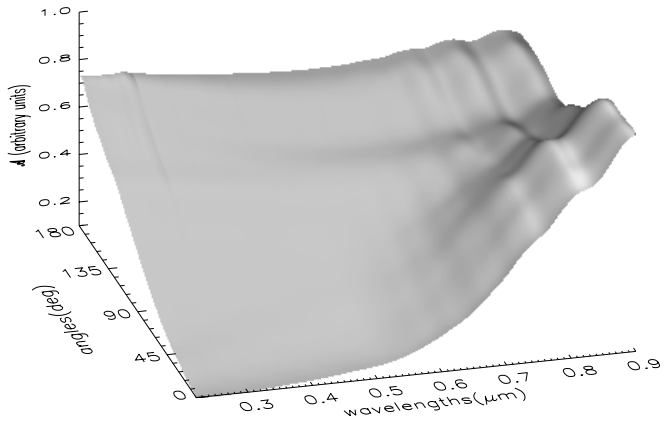

Fig. 6. Form factor $\mathcal{A}(\lambda, \lambda', a, \theta, \theta_d)$: incident wavelength $\lambda = 220$ nm, sphere radius $a = 1000$ nm (size parameter $x \sim 28.6$, near geometric optics limit).

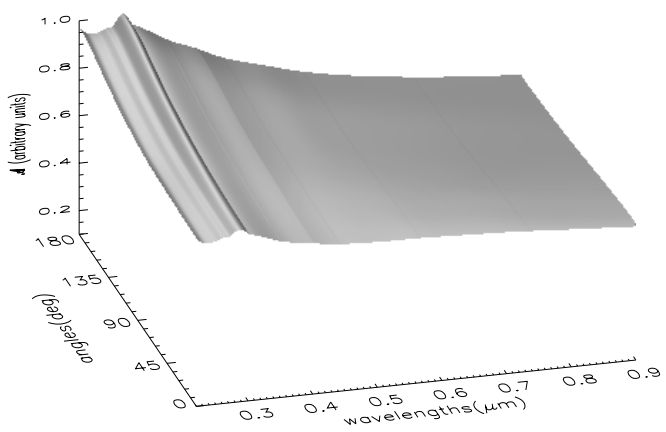

Fig. 7. Form factor $\bar{\mathcal{A}}(\lambda, \lambda', \theta, \theta_d)$: incident wavelength $\lambda = 220$ nm, weighted average over a size distribution $n(a) \propto a^{-3.5}$ with 10 nm $\leq a \leq 1000$ nm.

$n(a) \propto a^{-3.5}$, with 10 nm $\leq a \leq 1000$ nm (see e.g. Mathis et al. 1977) and using the complex refractive index (reproduced in Fig. 2) of the processed organic refractory residue taken from Jenniskens (1993). Figure 7 shows the resulting effective $\bar{\mathcal{A}}(\omega, \omega', \theta, \theta_d)$. From the comparison between Figs. 3 through 6 and Fig. 7, we see that, as expected, the interference pattern was washed out and, at first sight, the behaviour is apparently very similar to the one in the Rayleigh limit (see Fig. 3). This is not unexpected, since the chosen distribution is dominated by smaller particles. However, upon closer inspection, we see that $\bar{\mathcal{A}}(\omega, \omega', \theta, \theta_d)$ retains a marked dependence on the angle θ, which is absent in the Rayleigh limit and is instead inherited from larger sizes. The use of a distribution $n(a)$ with a different spectral index in the range from -3.3 to -3.6 does not qualitatively change the resulting $\bar{\mathcal{A}}(\omega, \omega', \theta, \theta_d)$. Changing the range of sizes, instead, can change the slope of $\bar{\mathcal{A}}(\omega, \omega', \theta, \theta_d)$ with respect to wavelength, if a large $a_{\min}$ is chosen, while still retaining its smooth appearance. This is clearly demonstrated in Fig. 8, in which $\bar{\mathcal{A}}(\omega, \omega', \theta, \theta_d)$ was computed for the same size distribution but with 150 nm $\leq a \leq 1000$ nm. For further clarity, Fig. 9 shows bi-dimensional excerpts from the surface plots in Figs. 7 and 8 for the forward ($\theta = 0°$) and backward ($\theta = 180°$) directions.

3. Astrophysical implications

Interstellar particles are obviously non-spherical, as evidenced e.g. by the observed polarisation of starlight; moreover, they are very unlikely to be homogeneous, as a consequence of their life-cycle which cyclically experiences very different ambient conditions, being subjected to the deposition (inside dense clouds) of frozen mantles, energetic processing by UV radiation and cosmic rays, sublimation of volatile components (in the diffuse medium), and grain-grain collisions leading to accretion and shattering.

Nonetheless, since a distribution of spherical, homogeneous dust particles *does* successfully reproduce many of the main observational characteristics of the interstellar extinction curve (see e.g. Mathis et al. 1977), we do expect our simple

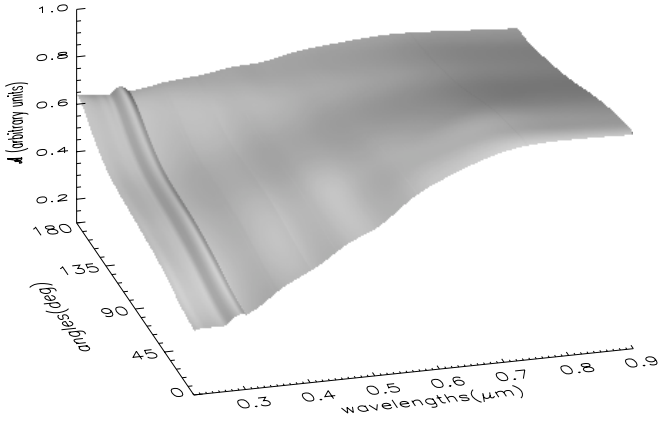

Fig. 8. Form factor $\bar{\mathcal{A}}(\lambda, \lambda', \theta, \theta_d)$: incident wavelength $\lambda = 220$ nm, weighted average over a size distribution $n(a) \propto a^{-3.5}$ with 150 nm $\leq a \leq 1000$ nm.

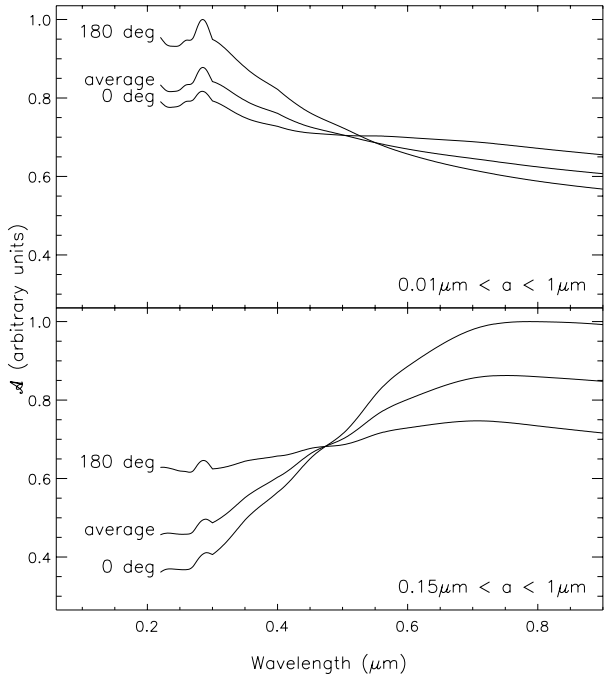

Fig. 9. Excerpts of Figs. 7 and 8 illustrating the spectral behaviour of $\bar{\mathcal{A}}(\omega, \omega', \theta, \theta_d)$ respectively at $\theta = 0°$, $\theta = 180°$ and averaged over angles. Both boxes refer to a weighted average of $\mathcal{A}(\omega, \omega', a, \theta)$ over a size distribution $n(a) \propto a^{-3.5}$, the top one with 0.01 μm $\leq a \leq 1$ μm, the bottom one with 0.15 μm $\leq a \leq 1$ μm.

model to exhibit, to the same extent, the main qualitative effects of dust grain geometry, self-extinction and self-absorption on their PL properties. Of course, more detailed and realistic models will be needed for their more precise quantitative evaluation, but still the present one is a first, important step in the right direction.

3.1. Dust particle rotation

Some of the astrophysical implications of the results of our simplified model are strongly related to the explicit angular dependence of the PL spectrum which we have obtained in our formulas. One basic question relevant from the astrophysical point of view is: "how much does a dust particle rotate in the time interval it spends between the absorption and the subsequent emission processes?". If the above rotation $\Delta\theta$ is large, the dust particle will lose all memory of the direction the exciting photon came from; in this case, the outgoing PL will be modulated by *the angular average* of $\mathcal{A}(\omega, \omega', a, \theta, \theta_d)$. If, on the other hand, this rotation is very small, the particle can be considered to be essentially "frozen" between absorption and emission, and the outgoing PL will be modulated by $\mathcal{A}(\omega, \omega', a, \theta, \theta_d)$, including its full angular dependence. In intermediate cases, one should consider a weighted angular average of $\mathcal{A}(\omega, \omega', a, \theta, \theta_d)$ over the distribution of rotation angles of the particle between absorption and emission.

To answer the above question, we may estimate the order of magnitude of the average $\Delta\bar{\theta}$ from the relation:

$$\Delta\bar{\theta} = \bar{\omega}_{\rm rot}\, \tau, \tag{3}$$

where τ is the typical decay time of an electronic transition involving emission of radiation, and $\bar{\omega}_{\rm rot}$ is the characteristic angular frequency of rotation of such a dust particle in interstellar conditions. In turn, we may estimate $\bar{\omega}_{\rm rot}$ considering the particle as a rigid rotating body with momentum of inertia I in thermal equilibrium with the kinetic temperature of the gas $T_{\rm gas}$:

$$\frac{1}{2} I\, \bar{\omega}_{\rm rot}^2 = k_{\rm B}\, T_{\rm gas}, \tag{4}$$

where $k_{\rm B}$ is the Boltzmann constant. The expression of the momentum of inertia of a homogeneous sphere in terms of its radius a and its density ρ_0 is given by:

$$I_{\rm sphere} = \frac{8\pi\rho_0}{15}\, a^5.$$

If we combine the above equation with Eqs. (3) and (4), we obtain:

$$\Delta\bar{\theta} = \bar{\omega}_{\rm rot}\, \tau = \left(\frac{15}{4\pi\rho_0}\right)^{1/2} \left(\frac{k_{\rm B} T_{\rm gas}}{a^5}\right)^{1/2} \tau,$$

which can be approximately expressed (in radians) by:

$$\Delta\bar{\theta} \sim 128.4 \left(\frac{\rm g/cm^3}{\rho_0}\right)^{1/2} \left(\frac{T_{\rm gas}}{K}\right)^{1/2} \left(\frac{\mu\rm m}{a}\right)^{5/2} \left(\frac{\tau}{\rm s}\right).$$

If we assume a temperature of the order of $T = 100$ K for the diffuse interstellar medium, a particle density of the order of 1 g/cm^3, and a decay time of the excited state of the order of 10^{-8} s, we get for $\Delta\bar{\theta}$ values of about 2.3×10^{-6}, 7.3×10^{-5}, 2.3×10^{-4} radians, for a ranging from 2, to 0.5 and 0.05 μm, respectively. In all these cases, the estimated $\Delta\bar{\theta}$ is much smaller than the scale of the detailed angular structure of $\frac{{\rm d}C_{\rm pl}}{{\rm d}\Omega {\rm d}\omega'}$, hence these particles can be considered to be effectively immobile between absorption and emission. In this case,

$\mathcal{A}(\omega, \omega', a, \theta, \theta_d)$, with no angular average, will be the function modulating the outgoing PL. We remark that the above still holds even for temperatures as high as $T \sim 10^4$ K, since $\bar{\Delta\theta} \propto T^{1/2}$, hence for a very wide range of physical conditions where the ERE is observed. For extremely small sphere radii, namely 0.005 μm = 5 nm, we obtain for $\Delta\bar{\theta}$ a value of about 7 radians which *does* produce a strong angular mixing in the emission process such that any memory of the direction of the exciting light is lost. However, such small particles will be in the Rayleigh limit anyway, for any reasonable optical constants; hence, in this specific case, $\mathcal{A}(\omega, \omega', a, \theta, \theta_d)$ shows no angular dependence anyway, and dust grain rotation makes no difference as far as the resulting PL is concerned.

Summing up, in a typical interstellar environment spherical particles in the range of sizes between 0.05 and 2 μm should not rotate appreciably between the absorption and subsequent emission of a photon, *provided that their rotation is in thermal equilibrium with the kinetic temperature of the gas*. In such a situation a memory of the direction of the incident radiation is conserved in the emission process, and an explicit knowledge of this dependence is fundamental in the application to PL phenomena originating from interstellar dust particles such as the ERE. Indeed, one of the properties of the ERE is that its spectral shape is observed to be different even in different positions of the same object (Witt & Boroson 1990; Perrin & Sivan 1992). Our work suggests that this effect may be at least partly due to the variation of the angle between the observation direction and the direction the exciting radiation comes from, something that was overlooked in previous analyses.

However, at least part of the dust grain particles have long been thought to rotate much faster than thermally: Purcell (1975, 1979) first thoroughly calculated the effects of the so called *rocket effect*, whereby inhomogeneities of a particle lead to torques which do not average to zero over time. A prototypical example of the rocket effect is dust-catalysed H_2 formation (Rouan et al. 1997). This effect was long thought to dominate suprathermal dust grain rotation, until Draine & Weingartner (1996) first provided a thorough calculation of radiative torques using the Discrete Dipole Approximation (DDA) for a model anisotropic particle, showing that these latter torques may even dominate those due to H_2 formation in the case of relatively large dust particles and/or strongly anisotropic radiation fields. More recently, T-matrix techniques were used to obtain the detailed inertial response of fluffy dust grains, including radiation pressure (Saija et al. 2003) and radiative torques (Borghese 2003). Other effects, such as birefringence with respect to different circular polarisations of light have been proposed as well (Dolginov & Mytrophanov 1976; Lazarian 1995). The overall balance of the effects which tend to spin up dust particles and dissipative effects which tend to spin them down was studied by Draine & Lazarian (1998). Summing up, the current state of the art of theoretical work as to dust grain rotation in the ISM seems to indicate that:

- very small dust particles (i.e. nanoparticles) may rotate subthermally due to efficient damping via microwave emission (Draine & Lazarian 1998);
- particles smaller than ~0.1 μm will rotate thermally, since neither radiative torques (Draine & Weingartner 1996) nor catalytic H_2 formation (Lazarian & Draine 1999) are able to significantly spin them up;
- particles larger than ~0.1 μm will be driven by radiative torques to rotational speeds which can exceed by a few orders of magnitude those expected in thermal equilibrium conditions ("suprathermal" rotation) (Draine & Weingartner 1996).

In principle, therefore, for dust particles larger than ~0.1 μm rotational speeds might be large enough to wash out at least some of the angular dependence of $\mathcal{A}(\omega, \omega', a, \theta, \theta_d)$.

While such suprathermal rotation of interstellar dust grains has a strong theoretical foundation and is believed to be important in several astrophysical conditions, there is no direct observational evidence to date of its existence. Our model predicts a direct consequence of suprathermal rotation of dust grains in astronomical PL phenomena such as ERE, which would be amenable to direct testing.

3.2. Dust grain size effects

Apart from the dependence of the emitted spectrum on the angle of observation, our model shows that both $\mathcal{A}(\omega, \omega', a, \theta, \theta_d)$ and its integral over angles have a strong dependence on the radius of the dust particle. In particular, $\mathcal{A}(\omega, \omega', a, \theta, \theta_d)$ shows two strongly different types of behaviour with respect to the emission wavelength, depending on dust grain size:

- In the Rayleigh limit self-absorption in the dust particle is negligible, whereas it is *not* negligible for the experimental configuration assumed ($\theta_d = 30°$, see Fig. 1). This means that in Eq. (2) only $\gamma_0 \neq 0$, and it shows a weak dependence on the emission wavelength; this, in turn, means that the behaviour of $\mathcal{A}(\omega, \omega', a, \theta, \theta_d)$ with respect to emission wavelength is governed by $g(\omega, \omega')$, which expresses the self-absorption in the laboratory sample and, in this case, increases with decreasing wavelength. Summing up, in the Rayleigh limit $\mathcal{A}(\omega, \omega', a, \theta, \theta_d)$ is independent of θ and *decreases* with increasing emission wavelength.
- For somewhat larger dust particle sizes, self-absorption becomes more and more important in the grain, and reverses the above behaviour, so that $\mathcal{A}(\omega, \omega', a, \theta, \theta_d)$ *increases* with emission wavelength.

This behaviour is not limited to particles of specific sizes, but remains very evident also for different distributions of particle sizes, as clearly shown by the comparison of Figs. 7 and 8 and of the top and bottom boxes of Fig. 9.

The above discussion hints that, for the adopted behaviour of the complex refractive index, larger particles generally display a form factor $\mathcal{A}(\omega, \omega', a, \theta, \theta_d)$ which becomes larger for increasing wavelengths, and therefore they are able to move the observed PL peak red-wards, regardless of dust grain rotation.

In particular, one could therefore suggest, for example, that the peak of the ERE in different regions of the Red Rectangle (Witt & Boroson 1990) changes in part due to a variation in the

distribution of particle sizes, with increasingly large particles near the source which powers the nebula.

4. Conclusions

This overly simplified application of our model, even with its acknowledged limitations, still provides a very important improvement over neglecting particle size dependent self-absorption effects altogether, as almost all studies comparing the ERE with laboratory data on the PL of carbonaceous materials did so far. While we consider it would be hazardous to draw definitive conclusions from the present indicative results, nonetheless some rather strong points can be safely made:

- Self-absorption and geometric effects *must* be taken into account when comparing laboratory PL data taken on macroscopic samples with the observed PL from small particles, since they can have an important effect.
- We suggest that the major objections against the hypothesis of HAC as the carrier of the ERE, namely that it is impossible to simultaneously match both the spectrum and the efficiency of the observed PL, must be reexamined in the light of the results presented here: either appropriate laboratory measures should be made *directly* on small particles similar in size and structure to the ones believed to be present in astrophysical environments, or a theoretical model like the one we presented should be used to bridge the gap between the macroscopic laboratory samples and the interstellar dust grains. Indeed, our present work hints that small particle effects would make the PL arising from dust grains considerably redder, maybe enough to bring the PL spectrum arising from highly hydrogenated HAC into acceptable agreement with ERE observations, while still preserving their high quantum efficiency. For a definitive assessment of this possibility the present model will need to be generalised to more realistic dust particles.
- Carbonaceous dust particles, which are included essentially in all dust models, must be strongly photoluminescent in environments where they are hydrogenated, such as in PDRs, and thus their expected emission must be at least *compatible* with ERE, or the models will need to be revised accordingly.

Acknowledgements. G. Malloci acknowledges the financial support by INAF - Osservatorio Astronomico di Cagliari. The authors are thankful to Prof. C. V. M. Van der Mee for his help with generalised spherical functions theory, and Dr. C. Cecchi-Pestellini and Prof. F. Borghese for their suggestions and helpful discussions, and the referee for his/her useful comments.

References

Borghese, F. 2003, private comunication
Chlewicki, G., & Laureijs, R. J. 1987, in Polycyclic aromatic hydrocarbons and astrophysics, ed. A. Legèr, L. d'Hendecourt, & N. Boccara, Proc. NATO Advanced Research and CNRS Workshop, Les Houches France, Feb. 17–22, 1986 (Dordrecht: D. Reidel Publishing), 335
Darbon, S., Perrin, J. M., & Sivan, J. P. 1998, A&A, 333, 264
Dolginov, A. Z., & Mytrophanov, I. G. 1976, Ap&SS, 43, 291
Draine, B. T., & Lazarian, A. 1998, ApJ, 508, 157
Draine, B. T., & Weingartner, J. C. 1996, ApJ, 470, 551
Duley, W. W. 1985, MNRAS, 215, 259
Furton, D. G., & Witt, A. N. 1990, ApJ, 364, L45
Furton, D. G., & Witt, A. N. 1992, ApJ, 386, 587
Gordon, K. D., Witt, A. N., & Friedmann, B. C. 1998, ApJ, 498, 522
Guhathakurta, P., & Tyson, J. A. 1989, ApJ, 346, 773
Jenniskens, P. 1993, A&A, 274, 653
Lazarian, A. 1995, MNRAS, 274, 679
Lazarian, A., & Draine, B. T. 1999, ApJ, 516, L37
Ledoux, G., Ehbrecht, M., Guillois, O., et al. 1998, A&A, 333, L39
Ledoux, G., Guillois, O., Huisken, F., et al. 2001, A&A, 377, 707
Léger, A., Boissel, P., & d'Hendecourt, L. 1988, Phys. Rev. Lett., 60, 921
Li, A., & Greenberg, J. M. 1997, A&A, 323, 566
Malloci, G. 2003, Ph.D. Thesis, Università degli Studi di Cagliari
Malloci, G., Mulas, G., & Benvenuti, P. 2004, A&A, 420, 809
Mathis, J. S., Rumpl, W., & Nordsieck, K. H. 1977, ApJ, 217, 425
Mathis, J. S., & Whiffen, G. 1989, ApJ, 341, 808
Mattila, K. 1979, ApJ, 78, 253
Perrin, J. M., Darbon, S., & Sivan, J. P. 1995, A&A, 304, L21
Perrin, J. M., & Sivan, J. P. 1992, A&A, 255, 271
Pierini, D., Majeed, A., Boroson, T. A., & Witt, A. N. 2002, ApJ, 569, 184
Purcell, E. M. 1975, in The Dusty Universe, 155
Purcell, E. M. 1979, ApJ, 231, 404
Robertson, J. 1996, Phys. Rev. B, 53, 16303
Rouan, D., Leger, A., & Le Coupanec, P. 1997, A&A, 324, 661
Saija, R., Iatì, M. A., Giusto, A., et al. 2003, MNRAS, 341, 1239
Sakata, A., Wada, S., Narisawa, T., et al. 1992, ApJ, 393, L83
Schmidt, G. D., Cohen, M., & Margon, B. 1980, A&A, 239, L133
Scott, A. D., Evans, A., & Rawlings, J. M. C. 1994, MNRAS, 269, L21
Seahra, S. S., & Duley, W. W. 1999, ApJ, 529, 719
Sivan, J., & Perrin, J. 1993, ApJ, 404, 263
Szomoru, A., & Guhathakurta, P. 1998, ApJ, 494, L93
Watkin, S., Gledhill, T. M., & Scarrott, S. M. 1991, MNRAS, 252, 229
Webster, A. 1993, MNRAS, 264, L1
Witt, A. N., & Boroson, T. A. 1990, ApJ, 355, 182
Witt, A. N., Gordon, K. D., & Furton, D. G. 1998, ApJ, 501, L111
Witt, A. N., & Malin, D. F. 1989, ApJ, 347, L25
Witt, A. N., & Schild, R. E. 1988, ApJ, 325, 837
Witt, A. N., Stecher, T. P., Boroson, T. A., & Bohlin, R. C. 1989, ApJ, 336, L21